The Mechanical Behaviour of Ultra Fine Grained Titanium Alloys at High Strain Rates

N. Herzig[1], L.W. Meyer[1], D. Musch[1], T. Halle[1], V.A. Skripnyak[2], E.G. Skripnyak[2], S.V. Razorenov[3], L. Krüger[4]

[1] Chemnitz University of Technology, Materials and Impact Engineering, Germany
[2] Tomsk State University, Russia
[3] Russian Academy of Sciences, Institute of Problems of Chemical Physics, Chernogolovka, Russia
[4] Technical University Bergakademie Freiberg, Institut für Werkstofftechnik, Germany

Abstract

Within this study the mechanical behaviour of ultra-fine grained Ti-6-22-22S titanium alloy was investigated and compared to coarse grained material. By severe plastic deformation using the cyclic channel die compression process, grain sizes between 300 and 500 nm were obtained. The mechanical behaviour was studied over a wide range of strain rates from 10^{-3} - 10^{7} s-1 under compressive loading using different experimental techniques. A significant increase of flow stress with decreasing grain size compared to the coarse grain state was found. An evaluation of the strain hardening behaviour of the UFG material shows a significant increase of the strain hardening coefficient at high strain rates for low plastic deformation. The strain rate sensitivity of the material is found to be constant within a range of strain rates from 10^{-3} to 10^{6} s^{-1} but increases at higher plastic strains. However, compressive deformability is nearly constant up to 10^{2} s^{-1} and decreased disproportionately at higher rates of strain. With decreasing grain size a significant decrease of compressive deformability was found. The strength at failure is increased with increasing strain rate.

Keywords

Impact, high strain rate, ultra-fine grain, material

1 Introduction

During the last decade, considerable efforts have been made to produce ultra-fine grained (UFG) titanium alloys due to their advantages of enhanced strength at room temperature and large deformability at elevated temperatures [1]-[4]. UFG α and α+β titanium alloys

are usually produced by various Severe Plastic Deformation (SPD) methods, such as Equal Channel Angular Pressing (ECAP), High Pressure Torsion (HPT), Twist Extrusion (TE), and Multi-Directional Forging (MDF) [5]. These methods allow receiving bulk UFG materials with a grain size down to 100 nm in diameter.

The earlier research on the mechanical behaviour of UFG titanium has shown that decreasing grain size leads to a significant increase of the yield strength, hardness, and ultimate strength but to a decrease of the strain at fracture [1]-[4]. However, mechanical properties of UFG titanium alloys under dynamic loading conditions are poorly investigated. A strong increase of the yield stress of UFG α titanium alloy VT1-0 at strain rates of 10^5 to 10^6 s^{-1} and strain hardening under shock compression loading have been shown e.g. in [6].

The objective of this research is to investigate the mechanical behaviour of UFG $\alpha+\beta$ titanium alloy (Ti-6-22-22S) within a range of strain rates from 10^{-3} up to 10^7 s^{-1} and to analyse the strain hardening behaviour, the strain rate sensitivity of the flow stress and dynamic strength compared to coarse grained material state, which was investigated in wide ranges of strain rates and temperature e.g. in [8].

2 Material and methods

2.1 Material

Within this study the $\alpha+\beta$ titanium alloy Ti-6-22-22S (Ti-6Al-2Sn-2Zr-2Cr-2Mo-Si) was investigated in two different states. Its chemical composition is shown in Table 1.

element	Al	Sn	Zr	Mo	Cr	Si	Fe	O	N	C
wt.-%	5.75	1.96	1.99	2.15	2.10	0.13	0.04	0.082	0.006	0.009

Table 1: *Chemical composition of Ti-6-22-22S (wt.-%)*

The material was studied using two different grain sizes. For the initial material state a grain size of 10 µm was observed. Additionally, the material was used in ultra-fine grained state. To reduce grain size and to obtain a nanostructured material the titanium alloy was processed by Cyclic Channel Die Compression technique (CCDC) at elevated temperatures. Due to tool design the specimen after a deformation step shows the same geometry like in initial state. Hence, the identical device can be used for several deformation steps. Performing the process according to route I or II (Fig. 1) different microstructures are observed. Hence, an accumulated plastic strain of >100% leads to a nanostructured material with a grain sizes between 300 and 500 nm. However, a non homogenous microstructure was found within a surface layer of 1 to 3 mm thickness and has to be removed before specimen manufacturing.

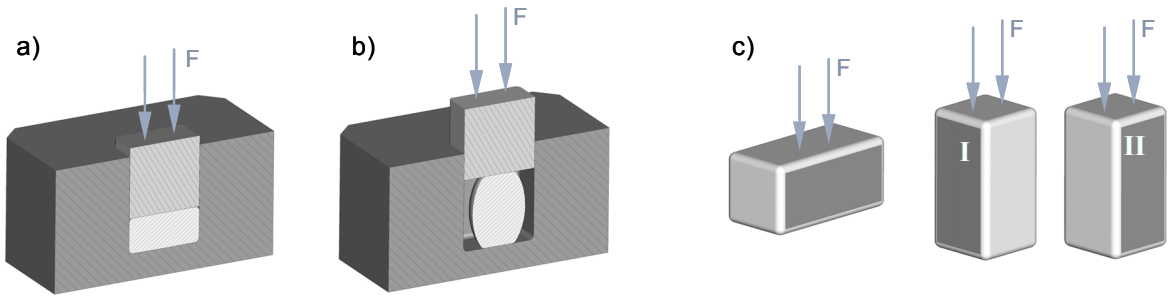

Figure 1: *Cyclic Channel Die Compression technology to produce UFG materials: (a) first and (b) second deformation step, (c) two different deformation routes*

2.2 Methods

To investigate the mechanical behaviour of coarse grained and UFG Ti-6-22-22S alloy, a variety of different testing facilities were used. The material was studied under compressive and shock loading conditions within a range of strain rates from 10^{-3} to 10^{7} s^{-1} at room temperature. Quasistatic tests were performed using a servohydraulic machine. Force was measured by a calibrated load cell. The strain response was obtained either by the use of strain gauges up to limited strains of maximum 8% plastic strain or by inductive sensors for higher deformations.

Dynamic tests at strain rates of 10^{2} s^{-1} were done using a drop weight tower device [8]. A guided mass of 600 kg impacts the specimen at a velocity of approximately 1.5 m/s and leads to deformation of the material. The force during testing is calculated from the elastic deformation of the punch obtained by strain gauges and the use of Hooke's law. The deformation was measured either by strain gauges or incremental gauges. Dynamic tests at strain rates from 10^{3} to 10^{4} s^{-1} were done using the Split Hopkinson Pressure Bar (SHPB) technique. The stress-strain response of the material is calculated using the theory of one dimensional wave propagation effects [9]. For the compression tests, cylindrical specimens with an initial diameter of Ø6 mm and an aspect ratio (ratio of specimen diameter to specimen height) of 1 were used.

Shock loading experiments were realised by Flyer Plate Impact (FPI) tests [10]. The experimental setup is shown in Fig. 2. An impactor is accelerated by an explosive lens and impacts the specimen. Hence, a planar shock wave is induced and travelling through the specimen. From measurement of the free surface velocity by using a VISAR laser Doppler velocimeter, the dynamic yield strength is calculated. The output VISAR signals were recorded with a high-frequency digital oscilloscope with a time resolution of approximately 1 ns.

Hence, applying the evaluation method described e.g. in [11] and [12], a comparison of high rate data with the mechanical behaviour at lower strain rates can be made. Within this study specimen thicknesses between 0.67 and 10 mm were used, whereby the larger specimens of 6.36 and 10 mm thickness were impacted by 2 mm aluminium plates at 660±20 m/s. For impact velocities of 1250±50 m/s specimen thicknesses of 0.67 mm and 0.835 mm and aluminium plates with 0.1 to 0.12 mm in thickness were used. The measurement accuracy of free surface velocity was better than ±5 m/s independently of its peak value. Hence, the free surface velocity histories were used for determination of

the mechanical behaviour of the UFG titanium alloy under shock compression loading. Additionally, the free surface velocity history contains information on strain hardening and strain rate effects.

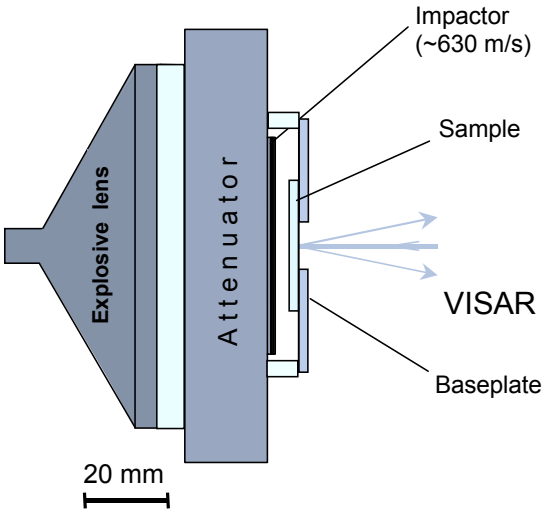

***Figure 2**: Experimental setup of flyer plate impact tests*

3 Results and discussion

3.1 Quasistatic and dynamic loading

Fig. 3 shows the stress-strain behaviour of the coarse grain and UFG titanium alloy under compressive loading at different strain rates. It can be clearly seen that with increasing strain rate an increase of flow stress for both materials can be found. For the coarse grained material a thermally activated flow stress increase in the order of 500 MPa compared to 400 MPa for the UFG state from 10^{-3} to 10^{3} s^{-1} is observed. Additionally, a significantly higher initial flow stress can be measured with decreasing grain size from 10 µm to 300 nm. Both material states tend to fail during compressive deformation under quasistatic as well as under dynamic loading conditions. However, a strong decrease of strain at fracture with decreasing grain size and increasing strain rate was observed.

From Fig. 3 a different strain hardening behaviour for the two materials can be observed. Defining the strain hardening coefficient n as the partial derivation of log σ by log ε (Eq. 1) a decrease of n with increasing strain rate is observed. Due to conversion of plastic work to heat under dynamic loading conditions thermal softening effects lead to a decrease of value n with increasing strain. However, failure initiation and occurrence lead to negative values of strain hardening coefficient which has no physical meaning but it can be used as a phenomenological value defining the start of fracture process.

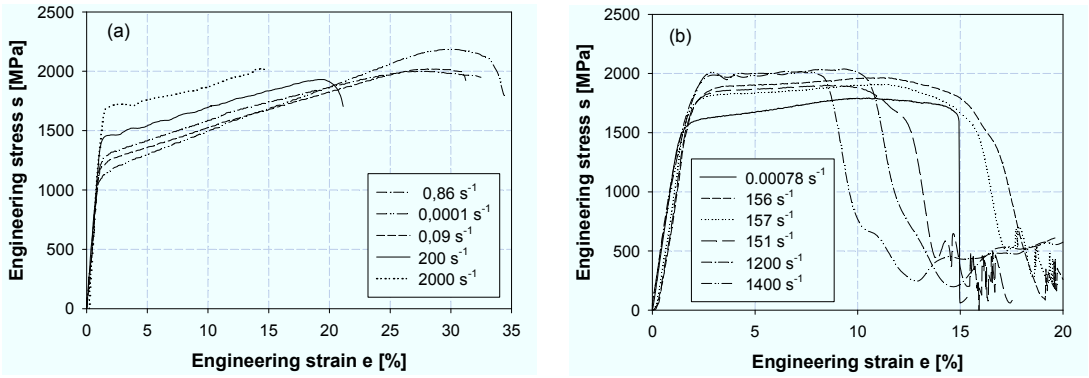

Figure 3: *Engineering stress – strain behaviour of (a) coarse grained and (b) UFG Ti-6-22-22S under compressive loading at different strain rates*

$$n = \left.\frac{\partial(\log\sigma)}{\partial(\log\varepsilon)}\right|_{\varepsilon} \tag{1}$$

Fig. 4 summarises the strain hardening coefficient for the coarse grain and UFG titanium alloy. Comparing coarse and ultra-fine grained material different strain hardening behaviour can be found. At the onset of plastic deformation the UFG material shows a 2.5 times higher strain hardening coefficient compared to the material with a grain size of 10 µm. During deformation the n-value is nearly constant for coarse grained material until failure process is initiated. The UFG material shows a strong decrease of strain hardening after low amount of plastic deformation. However, at higher strains nearly no hardening was found.

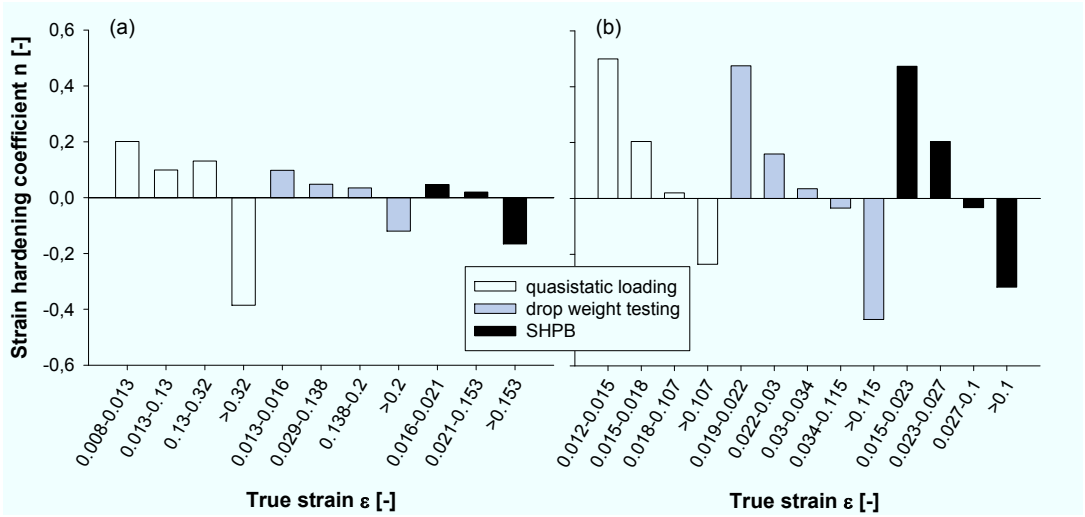

Figure 4: *Development of strain hardening coefficient with increasing deformation at different strain rates for (a) coarse grain and (b) UFG Ti-6-22-22S alloy*

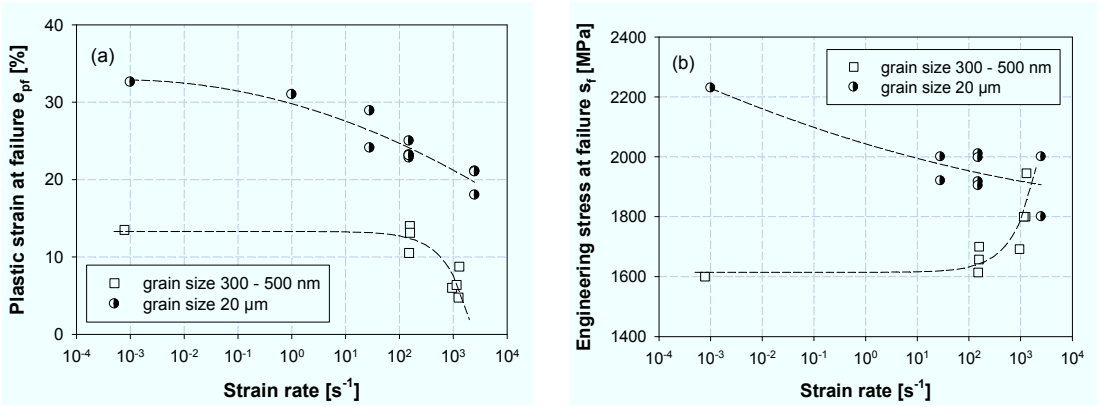

Figure 5: *(a) compressive deformability and (b) stress at failure of coarse and ultra-fine grained Ti-6-22-22S*

Fig. 5a illustrates compressive deformability of both material states. It can be seen that UFG material at room temperature is less deformable under compressive loading than coarse grain state. The plastic strain at failure is reduced at quasistatic loading from e_{pf} = 32% to 13 %. The material with 10 µm grain size shows a continuous decrease of compressive deformability with increasing strain rate, whereby the deformability behaviour of the UFG material is assumed to be nearly constant over a wide range of strain rates up to 10^2 s^{-1}. However, at higher strain rates a strong decreasing fracture strain was found. From Fig. 5b the stress at failure can be evaluated. It can be seen that coarse grained and UFG Ti-6-22-22S alloy show different behaviour. The material with a grain size of 10 µm shows a decrease of compressive strain at failure with increasing strain rate. For the UFG material the opposite behaviour was determined.

3.2 Impact loading by shock waves

Fig. 6 shows the free surface velocity history profiles measured by VISAR technique. Both material states, coarse grain and ultra fine grain, were tested with an impact velocity of ~650 and ~1250 m/s. It can be seen clearly that with increasing impact velocity increased free surface velocities are measured. The initial density of the titanium alloy was determined to 4.53 g/cm³, and the Poisson's ratio ν is 0.327. The longitudinal and the bulk sound velocities c_l and c_b are 6.01±0.04 km/s and 4.87±0.04 km/s, respectively. The amplitudes of shock waves were determined to 4.9 and 11.2 GPa for 10 µm grain size and 5.1 and 8.82 GPa for 300 nm grain size, respectively. For low impact velocity of ~650 m/s a higher value of Hugoniot Elastic Limit (HEL) σ_{HEL} for coarse grained Ti-6-22-22S was found, which was 260 MPa larger compared to UFG material. At impact velocities of ~1250 m/s the σ_{HEL} of UFG material was 400 MPa higher than for the as received state. The results are summarised in Tab. 2.

Additionally, from Fig. 6 the change of free surface velocity at spall Δu_{fs} can be determined. Δu_{fs} is evaluated as the difference between maximum of u_{fs} and the first valley after peak pressure. Hence, the spall strength σ^* was found to decrease for ultra fine grained material compared to coarse grain state. However, the difference in spall strength between the two material states increases at higher impact velocities (Tab. 2).

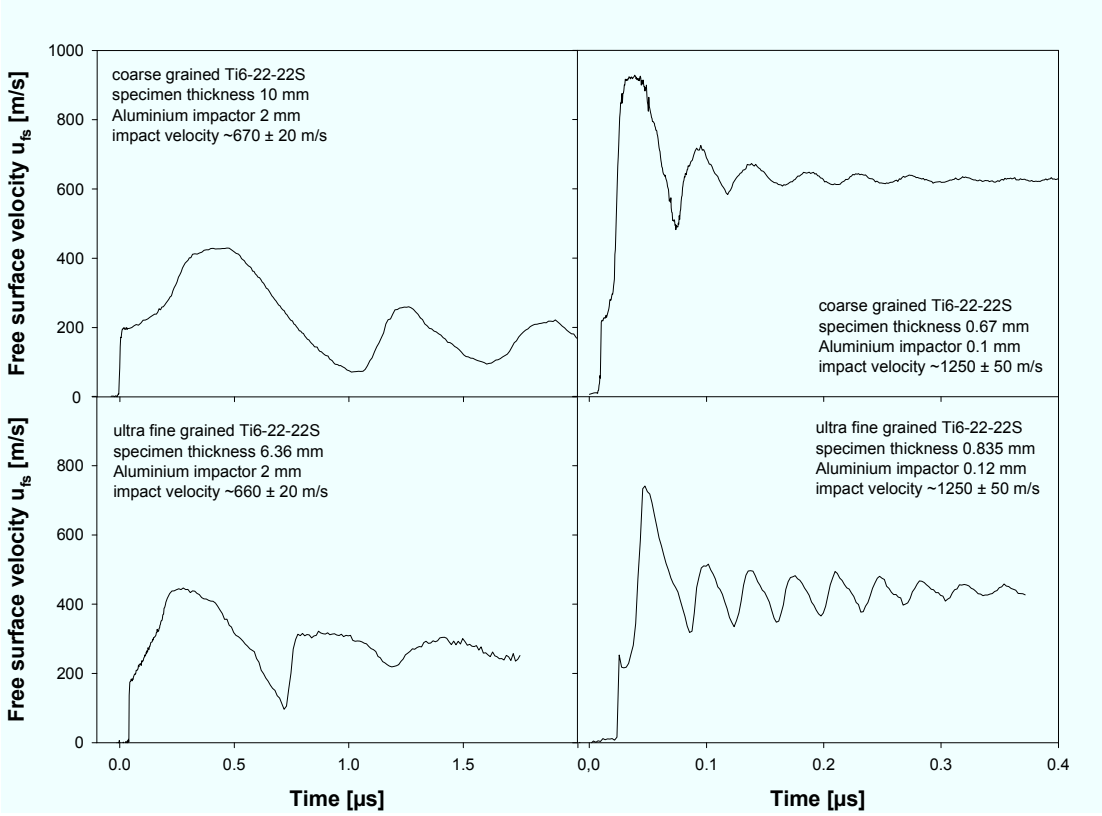

Figure 6: *Free surface velocity profiles for coarse grained and ultra fine grained Ti-6-22-22S alloy for two different impact velocities*

material	p_{max} [GPa]	σ_{HEL} [GPa]	$\sigma_{0.2}$ [GPa]	$\sigma_{0.5}$ [GPa]	σ_Y [GPa]	$h_{sp.}$ [mm]	$\dot{\varepsilon}$ 10^5 [s^{-1}]	σ^* [GPa]
cg Ti-6-22-22S	4.9	2.68	1.59	1.68	1.38	2.62	0.78	4.48
UFG Ti-6-22-22S	5.1	2.42	1.55	1.75	1.24	1.76	0.97	4.37
cg Ti-6-22-22S	11.2	3	1.81	1.93	1.55	0.17	14	5.55
UFG Ti-6-22-22S	8.82	3.4	1.8	1.92	1.75	0.16	11	5.13

Table 2: *Results of flyer plate impact experiments on Ti-6-22-22S*

To ensure comparability of impact results with quasistatic and dynamic compression tests the stress-strain response of the material have to be calculated. Therefore, the free surface velocity history profile $u_{fs}(t)$ was analysed and an approach of $u_{fs}(t) = 2u_p(t)$ and $d\sigma(t) = \rho a_\sigma \cdot du_p(t)$ was used. From the recalculated stress history profile the strain increment $d\varepsilon_x$ and the resolved shear stress τ were calculated. Assuming the uniaxial flow stress to be twice the shear stress, the stress-strain diagram of the material under shock loading can be drawn (Fig. 7). It must be emphasised that values of plastic strain under shock wave loading were less than 4%. However, at plastic strains larger than 1%,

obtained in shock loading experiments, softening effects have a strong influence on the measured material behaviour.

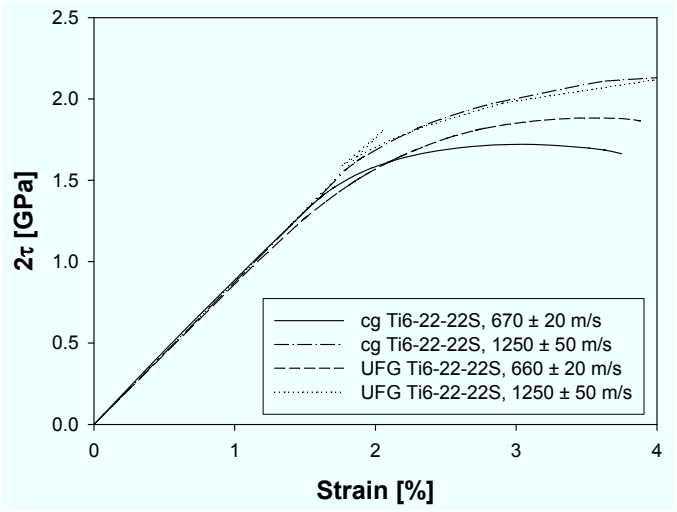

Figure 7: *Evaluation of stress-strain response of coarse grained and ultra fine grained Ti-6-22-22S alloy obtained under shock wave loading conditions.*

From Fig. 7 the 0.2% and the 0.5% flow stresses can be evaluated. Hence, for the 0.2% flow stresses similar results for both material states were observed. For larger strains, a significantly higher flow stress for UFG material at impact velocities of ~650±20 m/s compared to coarse grain material was found. However, the different flow stress behaviour for the two material states observed under uniaxial compression tests cannot be confirmed at shock wave loading conditions.

The results on flow stress behaviour of coarse grained and ultra-fine grained Ti-6-22-22S are summarised in Fig. 8. The 0.2% and 0.5% yield stress versus strain rate are shown.

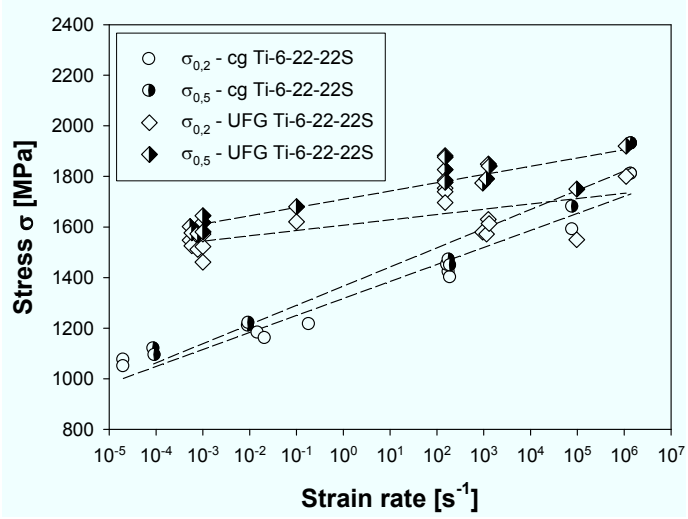

Figure 8: *Initial flow stress behaviour of coarse grained and ultra fine grained Ti-6-22-22S alloy over a range of strain rates from 10^{-4} to 10^{7} s^{-1}*

It can be seen that with decreasing grain size from ~10 µm to ~300 nm an increase of flow stresses can be measured. Under quasistatic loading conditions this difference was about 400 MPa. However, with increasing strain rate the difference between flow stresses of coarse grain and UFG material decreases, and under shock wave loading conditions nearly no different flow stresses were found. From Fig. 8 a linear dependence of flow stress on logarithmic strain rate can be evaluated for both materials. Even at high strain rates of $>10^4$ s^{-1} no alteration of strain rate sensitivity was found. Hence, the flow stress behaviour of coarse grained and ultra-fine grained Ti-6-22-22S can be assumed to be thermally activated within a range of strain rates ranging from 10^{-5} to $>10^6$ s^{-1}. Assuming the strain rate sensitivity of the material defined according to Eq. 2 different flow stress increasing increments per order of magnitude (oom) in strain rate can be found.

$$C = \left.\frac{\partial \ln \sigma}{\partial \ln \dot{\varepsilon}_p}\right|_{\varepsilon_p, T} \quad \left[\frac{MPa}{oom}\right] \tag{2}$$

	ε_p = 0.2%	ε_p = 0.5%
C_{UFG}	9.1	14.2
C_{cg}	29.2	32.9

Table 3: *Stress-strain rate sensitivity C of UFG and coarse grained Ti-6-22-22S*

In Tab. 3 the values of strain rate sensitivity obtained from Fig. 8 are shown. It can be clearly seen that ultra-fine grain Ti-6-22-22S is less sensitive on strain rate than coarse grained material. However, with increasing plastic strain, strain rate sensitivity was found to be increased.

4 Conclusions

From our work the following conclusions can be drawn:

1. Cyclic Channel Die Compression technology (CCDC) is an appropriate process to produce nanostructured titanium alloys. Grain sizes of 300 nm can be reached. However, CCDC process causes the formation of a non-homogeneous surface layer in the specimen. This layer should be removed before tests for characterising the mechanical behaviour of UFG materials.
2. Titanium alloy Ti-6-22-22S with grain sizes ~300 -500 nm shows a higher yield stress than the coarse-grained state (grain size 10 – 15 µm) within a wide range of strain rates. At quasistatic loading the UFG titanium alloy shows a 40% higher yield strength then commercial polycrystalline Ti-6-22-22S alloy.
3. The strain hardening behaviour of UFG titanium alloy differs significantly from coarse grained alloy. Within the first 1-1.5% of plastic strain, the UFG titanium alloy shows strong strain hardening which is more than at coarsed grain material. However, at larger plastic strains, no strain hardening was found for the UFG material.

4. The stress at Hugoniot elastic limit σ_{HEL} and flow stresses $\sigma_{0.2}$ and $\sigma_{0.5}$ of UFG titanium alloy at 10^6 – 10^7 s^{-1} are comparable to coarse grained material. No large difference between the two material states was found.
5. The compressive deformability of the UFG Ti 6-22-22S alloy is decreased at strain rates from 10^2 to 10^4 s^{-1} and is nearly constant at lower strain rates. However, the compressive deformability is reduced to one third and dynamically to one half of compressive failure strain of coarse grained Ti-6-22-22S.
6. For coarse grained material a decrease of compressive failure stress s_f was found. However, a different behaviour was measured for UFG material, where an increase of s_f in the order of 20% was observed.
7. For both material states a linear dependence of flow stress on logarithm of strain rate was found over the whole range of strain rates from 10^{-5} to $>10^6$ s^{-1}. However, the strain rate sensitivity is decreased with decreasing grain size. At shock wave loading the Hugoniot elastic limit and the yield stresses $\sigma_{0.2}$ and $\sigma_{0.5}$ of the UFG titanium alloy and their coarse grained counterpart are comparable.

References

[1] *Stolyarov, V.; Zhu, Y.T.; Alexandrov, I.V.; Lowe, T.C.; Valiev, R.Z.:* Grain refinement and properties of pure Ti processed by warm ECAP and cold rolling. Materials Science and Engineering, A343 (2003), 43-/50.

[2] *Ko, Y.G.; Shin, D.H.; Park, K.-T.; Lee, C.S.:* An analysis of the strain hardening behaviour of ultra-fine grained pure titanium. Scripta Mater., 54 (2006), 1785–1789.

[3] *Semenova, I.P.; Raab, G.I.; Saitova, L.R.; Valiev, R.Z.:* The effect of equal-channel angular pressing on the structure and mechanical behaviour of Ti 6Al 4V alloy. Materials Science and Engineering, A387–389 (2004), 805–808.

[4] *Sergueeva, A.V.; Stolyarov, V.V.; Valiev, R.Z.; Mukherjee, A.K.:* Superplastic behaviour of ultra-fine grained Ti–6Al–4V alloys. Materials Science and Engineering, A323 (2002), 318–325.

[5] *Valiev, R.Z.; Estrin, Y.; Horita, Z.; Langdon, T.G.; Zehetbauer, M.J.; Zhu, Y.T.:* Producing Bulk Ultrafine-Grained Materials by Severe Plastic Deformation. Journal of Material Science, April, 2006, 33-39.

[6] *Skripnyak, V.A.; Skripnyak, E.G.:* Shear strength of nanostructured and ultra-fine grained materials in shock waves. Phys. Mesomech., 2004, Vol. 7, P.1, 297-300.

[7] *Krüger, L.; Meyer, L.W.; Razorenov, S.V.; Kanel, G.I.:* Investigation of dynamic flow and strength properties of Ti-6-22-22S at normal and elevated temperatures. Int. J. of Impact Engineering, 2003, Vol. 28, 877-890.

[8] *Meyer, L.W.; Krüger, L.:* Drop-Weight Compression Shear Testing. ASM-Handbook, Vol. 8: Mech. Testing and Evaluation, ASM Int. Materials Park Ohio, 2002, 452-454.

[9] *Gray, G.T. (R.):* Classic Split-Hopkinson Pressure Bar Testing. ASM-Handbook, Vol. 8: Mech. Testing and Evaluation, ASM Int. Materials Park Ohio, 2002, 462-476.

[10] *Meyers, M.A:* Dynamic behaviour of materials. John Wiley & Sons, Inc., 1994.

[11] *Kanel, G.I.; Razorenov, S.V.; Fortov, V.E.:* Shock wave phenomena and the properties of condensed matter. Berlin-N.-Y, Springer-Verlag, 2004.

[12] *Antoun, T.; Seaman, L.; Curran, D.R.; Kanel, G.I.; Razorenov, S.V.; Utkin, A. V:* Spall fracture. Berlin-N.-Y, Springer-Verlag, 2003.